Reprinted from Preprint Volume: Conference on Cloud Physics and Atmospheric Electricity, July 31-August 4, 1978, Issaquah, Wash. Published by The American Meteorological Society, Boston, Mass.

4.10

# AIRBORNE MEASUREMENTS OF THE SIZE DISTRIBUTIONS OF PRECIPITATION PARTICLES IN FRONTAL CLOUDS

Robert A. Houze, Jr., Peter V. Hobbs, Paul H. Herzegh and David B. Parsons

Department of Atmospheric Sciences
University of Washington
Seattle, Washington

## 1. INTRODUCTION

In studies of the growth of precipitation, in cloud modeling and in radar meteorology, it is important to know the nature of the size distribution of the particles. Measurements of particle-size distributions have been made at ground level in rain (Marshall and Palmer, 1948; Geotis, 1968), snow (Imai *et al*, 1955; Gunn and Marshall, 1958; Ohtake, 1968) and hail (Douglas, 1964; Federer and Waldvogel, 1975). Many of these studies have been reviewed by Battan (1973). In general, they show that precipitation particle sizes are distributed according to the relation suggested by Marshall and Palmer (1948):

$$N(D) = N_o \exp(-\lambda D), \qquad (1)$$

where N(D)dD is the number of particles per unit volume of air with diameters between D and D + dD, and $N_o$ and $\lambda$ are constants. In certain special cases, important deviations from the Marshall-Palmer (MP) distribution have been noted (e.g., studies cited above indicate that in most situations, the MP distribution is a good approximation to the size distribution of precipitation particles at ground level for $D \gtrsim 1$ mm.

Measurements of the size distributions of precipitation particles above ground level are more scarce. However, evidence from airborne foil impactor measurements indicates a tendency for both raindrops (Merceret, 1974a,b; Cunning and Sax, 1977) and precipitation-sized ice particles (Simpson and Wiggert, 1971) to be distributed according to the MP distribution aloft as well as at ground level. This result has important implications for cloud modeling, for the validity of (1) aloft would justify the use of a microphysical parameterization scheme, such as first proposed by Kessler (1969), in which explicit calculation of the evolution of particle-size spectra is avoided by assuming that precipitation-sized particles are distributed according to (1) at all altitudes.

The advantage in using (1) to represent particle size distributions stems from its mathematical simplicity in integrals of the form

$$\int_0^\infty D^n N_o \exp(-\lambda D)dD = \Gamma(n+1)\lambda^{-n-1}, \qquad (2)$$

where $\Gamma$ is the Gamma Function, n is a real number > -1 and $\lambda > 0$. It follows from (1) and (2) that the total number of particles per unit volume of air $N_T$ is given by

$$N_T = \int_0^\infty N(D)dD = N_o\lambda^{-1}, \qquad (3)$$

the average diameter $\overline{D}$ of the particles by

$$\overline{D} = N_T^{-1}\int_0^\infty D\, N(D)dD = \lambda^{-1}, \qquad (4)$$

the variance $\overline{D'^2}$ of the diameters by

$$\overline{D'^2} = \overline{D^2} - \overline{D}^2 = N_T^{-1}\int_0^\infty D^2 N(D)dD - \lambda^{-2}$$

$$= 2\lambda^{-2} - \lambda^{-2} = \lambda^{-2}, \qquad (5)$$

and the mass of precipitation water per unit volume of air M by

$$M = \int_0^\infty \rho_D \frac{\pi}{6} D^3 N(D)dD = \rho_D \pi N_o \lambda^{-4} \qquad (6)$$

where $\rho_D$ is the density of a particle of diameter D. In (6) it is assumed that the particles are spherical.

We are particularly interested in whether the MP distribution holds aloft in the frontal clouds which we are investigating as part of the CYCLES (*Cyclonic Extratropical Storms*) PROJECT. If it does, then future efforts to model these cloud systems may be justified in assuming a microphysical parameterization scheme based on (1). In this paper, we present a study of the size spectra of precipitation particles measured aboard the National Center for Atmospheric Research's Sabreliner aircraft during the CYCLES PROJECT. These measurements are quite extensive, covering virtually the full range of temperatures aloft in frontal clouds, and they should be more precise than the foil impactor data of earlier airborne studies.

2. INSTRUMENTATION AND CALIBRATION PROCEDURES

Particle-size distributions were measured using a Particle Measuring Systems (PMS) cloud probe and a PMS precipitation probe (Knollenberg, 1970; Heymsfield, 1976) aboard the Sabreliner aircraft. The PMS probes automatically count the numbers of sampled particles whose diameters fall within each of fifteen size groups. The size groups for aggregate snow particles, which comprise most of the size spectra discussed here, range from 30 to 380 μm in the cloud probe and from 250 to 3120 μm in the precipitation probe. These sizes reflect a slight adjustment over nominal values, in order to correct for the probes' response to the irregular shapes of aggregate snow (Knollenberg, 1975).

Proper sizing of the sampled particles is further ensured by frequent instrument calibrations in which glass and metal spheres of known diameters are blown through the sampling volumes of the probes at high velocities, simulating in-flight sampling.

3. SYNOPTIC AND MESOSCALE SITUATIONS IN WHICH THE DATA WERE OBTAINED

The data in this study were obtained in the clouds associated with one occluded front and three cold fronts. In each of these cases, the precipitation was concentrated in mesoscale rainbands (Houze *et al.*, 1976), and the Sabreliner flew along horizontal tracks at various altitudes back and forth through the clouds associated with the rainbands. The PMS data were averaged to produce one particle-size spectrum for each horizontal pass across a rainband. A total of 38 such spectra were obtained. The temperature at flight altitude during these passes ranged from -42 to +6°C.

4. EXAMPLES OF PARTICLE-SIZE DISTRIBUTIONS

Some of the measured particle-size spectra fit the MP distribution very closely over the entire sampled size range (Fig. 1). In other spectra, however, a truncated MP distribution was observed (Figs. 2 and 3). The latter spectra deviated from the MP form at the smaller-particle end of the spectrum (that is for diameters less than or equal to some threshold value $D_o$) but were described very accurately by the MP distribution for particles with $D > D_o$. Table 1 shows that $D_o$ exceeded 1.5 mm in only one case and never exceeded 2 mm. Table 1 also indicates that two types of deviations occurred. The cases in which $D_o$ lay between 0 and 0.4 mm were characterized in the region $D \leq D_o$ by enhanced values of N(D) compared to the MP distribution fitting the large-particle ($D > D_o$) part of the distribution (Fig. 2). The cases in which $D_o$ lay between 0.4 and 2.0 mm were characterized in the region $D \leq D_o$ by suppressed values of N(D) compared to the MP distribution which fitted the large-particle part of the distribution (Fig. 3). Note further that this suppressed, rather flat, spectral region typically had a lower bound near D = 0.35 mm. Below this lower bound (N(D) increased rapidly with decreasing diameter.

The reason for the characteristic deviations from the MP spectrum at diameters $D \leq D_o$ in the truncated MP distributions, exemplified by Figs. 2 and 3, is not clear. Various explanations are plausible. We note that the truncated spectra were observed at temperatures lower than 0°C and that the PMS probes respond differently to different types of ice particles (Knollenberg, 1975). Possibly, then, the discontinuities in the observed spectra reflect boundaries between populations of different types of ice particles, or possibly between liquid and ice particles. As will be shown below in Fig. 5, liquid drops exhibit a flatter distribution (smaller λ) than do ice particles. Therefore, the flat spectrum in the suppressed type of deviation, such as the one seen in Fig. 3, could have been associated with super-

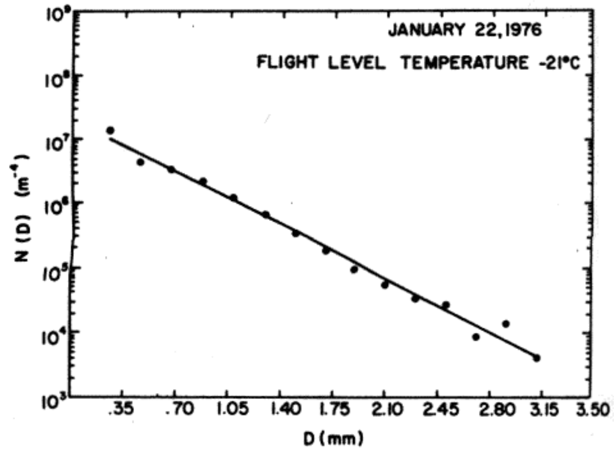


*Figure 1: Example of a measured particle-size spectrum which shows no significant deviation from a Marshall-Palmer distribution. N(D) is the concentration of particles per unit interval of diameter D. The Marshall-Palmer distribution best fitting the data is estimated by the indicated straight line which was computed by the method of least squares.*

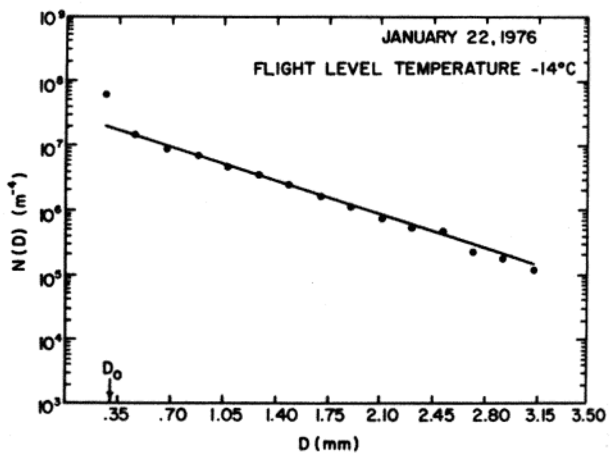


*Figure 2: Example of a measured particle-size spectrum which shows an enhanced type of deviation from a Marshall-Palmer distribution for diameters $D \leq D_o$. N(D) is the concentration of particles per unit diameter interval. The Marshall-Palmer distribution best fitting the data for diameters $D > D_o$ is estimated by the indicated straight line which was computed by the method of least squares.*

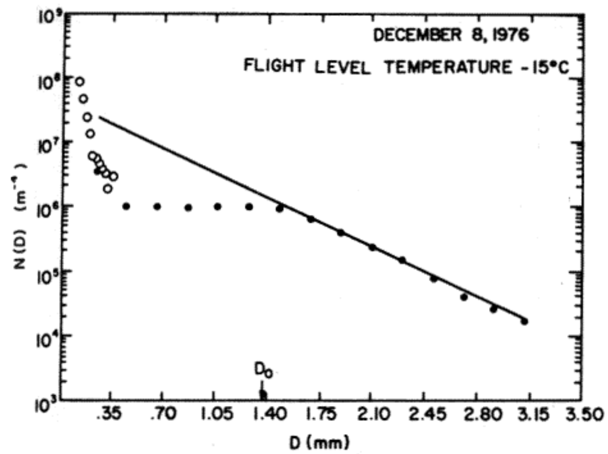


*Figure 3: Example of an observed particle-size spectrum which shows a large suppressed type of deviation from a Marshall-Palmer distribution for diameters $D \leq D_O$. N(D) is the concentration of particles per unit diameter interval. The dark circles indicate data from the PMS precipitation probe, while the open circles indicate data from the PMS cloud probe. The Marshall-Palmer distribution best fitting the data for diameters $D > D_O$ is estimated by the indicated straight line which was computed by the method of least squares.*

cooled water drops, while the larger particles in the region of $D > D_O$ may have been ice. Taking yet another point of view, we note that the suppressed type of deviation could have been due to evaporation of the relatively small particles in this region of the spectrum.

Whatever the reason for the deviations in the small-particle part of the observed spectra, the data in the region of $D > D_O$ show an excellent fit to the MP distribution. This fact was checked by using the method of least squares to fit straight lines to the observed spectra, since the MP distribution is a straight line in log-linear plots such as those in Figs. 1-3. Best-fit straight lines were computed both for spectra showing no deviation from the MP distribution (Fig. 1) and for the data in the region $D > D_O$ of spectra showing enhanced or suppressed deviations from an MP distribution at $D \leq D_O$ (Figs. 2 and 3). In every case, the magnitude of the correlation coefficient for the best-fit line was > 0.96.

We conclude, therefore, that each of the observed precipitation particle-size spectra was characterized by a basic MP distribution upon which other effects could be superimposed. These other effects sometimes caused deviations from the form of the MP distribution of smaller particle sizes, but the measured spectra always followed the MP form at diameters $D > D_O$. (We note that this result is consistent with the studies of particle-size spectra at ground level referred to in the Introduction; those studies showed the applicability of the MP distribution to surface precipitation only for $D \gtrsim 1$ mm.)

## 5. VARIATION OF PARTICLE-SIZE DISTRIBUTION PARAMETERS WITH TEMPERATURE

We now examine the parameters $N_O$ and $\lambda$ of the basic MP distributions characterizing the observed particle-size spectra. These parameters are indicated by the intercepts and slopes, respectively, of the computed straight lines described in Section 4. Although superimposed effects sometimes led to a deviation from the basic MP distribution in the small particle size range (Figs. 2 and 3), these effects did not prevent the basic MP spectra characterized by $N_O$ and $\lambda$ from behaving in a systematic way.

This systematic variation, illustrated in Figs. 4 and 5, can best be understood by first noting that according to Eqs. (3)-(5), $N_O\lambda^{-1}$ is the total concentration of particles and $\lambda^{-1}$ and $\lambda^{-2}$ are the mean and variance, respectively, of the basic MP distribution. The mean diameter $\lambda^{-1}$ (Fig. 4) shows a consistent increase with increasing temperature up to 0°C, at which temperature the values of $\lambda^{-1}$ discontinuously drop off by about an order of magnitude. This behavior is physically reasonable for a cloud in which ice particles form aloft at lower temperatures and grow by diffusional or collectional processes as they drift downward toward regions of higher temperature. The mean particle diameter ($\lambda^{-1}$) should thus increase with temperature until the particles reach the melting level. Passage through the melting level should be reflected as a sudden reduction in the mean particle size as the larger ice particles form smaller raindrops.

Obviously, the increase in the mean particle diameter ($\lambda^{-1}$) is accompanied by an increase in the variance ($\lambda^{-2}$) of the particle diameters with temperature above the melting level. This strong increase in the variance indicates that collectional processes (riming or aggregation) are active, leading to a broadening of the size distribution

*Table 1*

*Number of observed particle-size spectra which showed no deviation from an MP distribution, and the numbers exhibiting enhanced and suppressed types of deviations from an MP distribution for diameters* $D \leq D_O$.

| No deviation from MP distribution | Enhanced type of deviation | Suppressed type of deviation | | |
|---|---|---|---|---|
| | $D_O$ = 0 - 0.4 mm | $D_O$ = 0.4 - 1.0 | 1.0 - 1.5 | 1.5 - 2.0 mm |
| 9 | 13 | 6 | 9 | 1 |

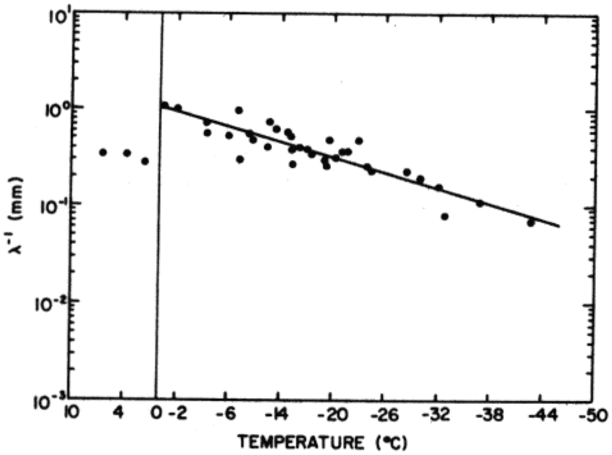


*Figure 4: Variation with temperature of the mean diameter ($\lambda^{-1}$) of the Marshall-Palmer distributions fitting the large-particle ($D > D_o$) part of all of the observed particle-size spectra. Best-fit line computed for temperatures < 0°C has a correlation coefficient of 0.90.*

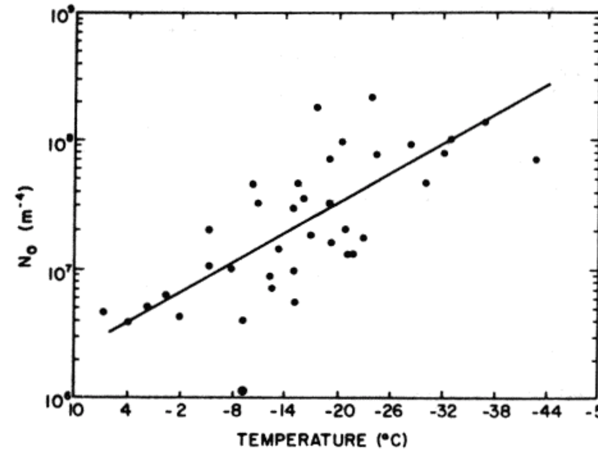


*Figure 5: Variation with temperature of the parameter $N_o$ of the Marshall-Palmer distributions fitting the large-particle ($D > D_o$) part of all of the observed particle-size spectra. Best fit line computed by the method of least squares has a correlation coefficient of -0.66.*

of ice particles as they drift downward at differing fallspeeds toward the melting level. As the ice particles pass through the 0°C level and melt to form much smaller raindrops, their size spectrum narrows.

The parameter $N_0$, which according to (1) can be interpreted as a measure of the concentration of small particles in the basic MP distribution, shows a consistent decrease with temperature (Fig. 5). This decrease indicates a diminution in the concentrations of smaller particles, again, probably as a result of collectional processes in which smaller particles are collected by the larger particles as they all drift downward toward the melting level.

The decrease of $N_0$ with temperature is offset, to some extent, above the melting level by the increase of $\lambda^{-1}$ to produce a comparatively slowly varying value of $N_T = N_0\lambda^{-1}$ (Fig. 6). That is, the total concentration of particles is very nearly conserved, varying by only a factor of about 2.7 between temperatures of -40 and 0°C, while $N_0$ and $\lambda^{-1}$ vary by nearly two orders of magnitude over the same temperature range. The reduction in the total concentration $N_T$ as the temperature increases is further evidence of the importance of collectional processes, in which a few big ice particles grow at the expense of the more numerous small particles to deplete the total concentration of particles somewhat faster than it can be replenished by nucleation at the ever higher temperatures to which the downward drifting particles are exposed.

The negative correlation of $N_0$ with temperature (Fig. 5) has more scatter than the positive correlation of $\lambda^{-1}$ with temperature above the melting level (Fig. 4). This additional scatter is to be expected from Eq. (6). Not only is $N_0$ inversely proportional to $\lambda^{-1}$, and hence to temperature according to the relation in Fig. 4, but $N_0$ is also directly proportional to the total precipitation water content M in the MP distribution. This relationship is confirmed by best-fit lines obtained after stratifying $N_0$ according to M (Fig. 7). The parameter $N_0$ is seen to increase with increasing values of M, and the magnitudes of the correlation coefficients corresponding to three of the four curves in Fig. 7 are greater than the one obtained in the general plot of $N_0$ versus temperature in Fig. 5, indicating that a better fit is obtained by taking into account M as well as temperature.

## 6. CONCLUSIONS

As part of the CYCLES PROJECT, measurements of the size distributions of precipitation particles have been made aboard an aircraft flying through the clouds associated with mesoscale rainbands in mid-latitude frontal systems at temperatures ranging from -42 to +6°C. The observed particle-size spectra tended to follow a basic MP distribution. Sometimes a deviation from this basic distribution occurred in the small-particle end of the observed spectra, but the basic MP form always dominated the spectra at diameters $\gtrsim$ 1.5 mm. The mean particle diameter ($\lambda^{-1}$) of the basic MP distribution and the variance ($\lambda^{-2}$) increased with increasing temperature above the melting level, while the parameter $N_0$ decreased with increasing temperature. Crossing the melting level, from lower to higher temperatures, produced an abrupt decrease in the values of $\lambda^{-1}$ and $\lambda^{-2}$.

We conclude from these findings that in extratropical cyclonic storms the precipitation in clouds associated with mesoscale rainbands tends to originate as ice particles aloft. As these ice particles drift downward toward the melting level they grow, accounting for the increase in $\lambda^{-1}$ with temperature above the 0°C level. Collection is apparently an important growth mechanism since the variance, or spread, of the MP distribution (indicated by $\lambda^{-2}$) also increases strongly with temperature above the melting level. The importance of the collection processes above the melting level is further

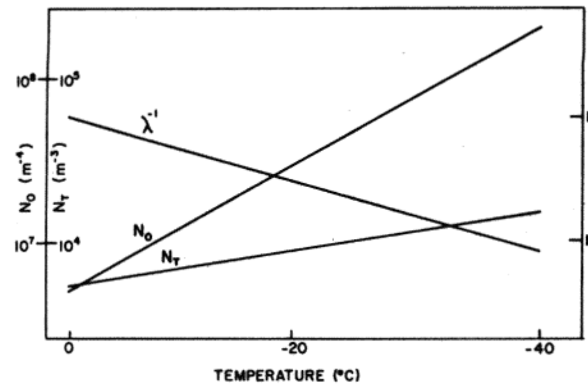


*Figure 6: Best-fit lines for $\lambda^{-1}$ and $N_O$ taken from Figs. 4 and 5 and their product, $N_T = N_O\lambda^{-1}$.*

indicated by decreases in $N_O$ (which indicates the concentration of small particles) and $N_T$ (the total particle concentration) with increasing temperature.

Passage of the precipitating particles through the melting level is accompanied by a sharp decrease in the mean particle size and spread of the basic MP distribution.

The tendency of precipitation and particles in the clouds associated with frontal rainbands to follow the MP size distribution over a wide range of temperatures aloft has important implications for future attempts to model these cloud systems. Parameterizations of cloud microphysics which assume an MP distribution in order to avoid explicit calculation of particle-size distributions appear now to have an empirical basis. Such parameterizations may well be essential to making tractable the problems of modeling complex frontal cloud systems.

*Acknowledgments:* This work was supported by the Meteorology Program of the Atmospheric Research Section of the National Science Foundation under Grants ATM74-14726A03 and ATM77-01344 and by the Air Force Office of Scientific Research under Grant No. F49620-77-C-0057. Thanks are due to all in the Cloud Physics Group for their hard work.

We thank members of the Research Flight Facility of the National Center for Atmospheric Research, which is sponsored by the National Science Foundation, for their help in operating the Sabreliner in the CYCLES PROJECT.

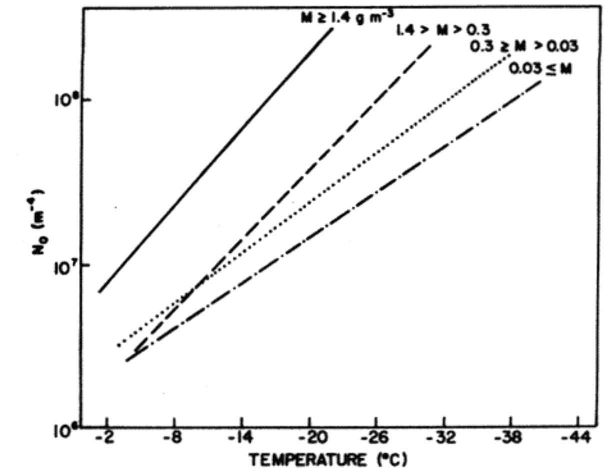


*Figure 7: Best-fit lines for $N_O$ obtained after subdividing the spectra according to the precipitation water content of the MP distributions associated with the observed particle-size spectra. Correlation coefficients for the four lines, in descending order of the indicated values of M, are -0.89, -0.66, -0.82 and -0.93.*

## REFERENCES

Battan, L. J., 1973: *Radar Observation of the Atmosphere*. University of Chicago Press, Chicago, 324 pp.

Douglas, R. H., 1964: Hail size distribution. *Proc. 11th Wea. Radar Conf.*, Amer. Meteor. Soc., Boston, 146-149.

Federer, B., and A. Waldvogel, 1975: Hail and raindrop size distributions from a Swiss multicell storm. *J. Appl. Meteor.*, 14, 91-97.

Cunning, J. B., and R. I. Sax, 1977: A Z-R relationship for the GATE B-scale array. *Mon. Wea. Rev.*, 105, 1330-1336.

Geotis, S. G., 1968: Drop-size distributions in eastern Massachusetts. *Proc. 13th Radar Meteor. Conf.*, Amer. Meteor. Soc., Boston, 154-157.

Gunn, K. L. S., and J. S. Marshall, 1958: The distribution with size of aggregate snowflakes. *J. Meteor.*, 15, 452-461.

Heymsfield, A. J., 1976: Particle size distribution measurement: an evaluation of the Knollenberg optical array probes. *Atmos. Tech.*, 2, 17-24.

Houze, R. A., P. V. Hobbs, K. R. Biswas, and W. M. Davis, 1976: Mesoscale rainbands in extratropical cyclones. *Mon. Wea. Rev.*, 104, 868-878.

Imai, I., M. Fujiwara, I. Ichimura and Y. Toyama, 1955: Radar reflectivity of falling snow. *Paper Meteor. Geophys. (Japan)*, 6, 130-139.

Kessler, E., 1969: On the distribution and continuity of water substance in atmospheric circulations. *Meteor. Monogr.*, No. 32, 84 pp.

Knollenberg, R. G., 1970: The optical array: an alternative to scattering or extinction for airborne particle size determination. *J. Appl. Met.*, 9, 86-103.

__________, 1975: The response of optical array spectrometers to ice and snow: a study of probe size to crystal mass relationships. Scientific Report No. 1, SCI75C0141-9875-001, Air Force Cambridge Research Labs., Hanscom AFB, Mass., 70 pp.

Marshall, J. S., and W. McK. Palmer, 1948: The distribution of raindrops with size. *J. Meteor.*, 5, 165-166.

Mason, B. J., and J. B. Andrews, 1960: Drop-size distribution from various types of rain. *Quart. J. Roy. Meteor. Soc.*, 86, 346-353.

Merceret, F. J., 1974a: A note on the distribution of raindrop-size spectra in Tropical Storm Felice. *Meteor. Mag.*, 103, 358-360.

__________, 1974: On the size distribution of raindrops in Hurricane Ginger. *Mon. Wea. Rev.*, 102, 714-716.

Ohtake, T., 1968: Change of size distribution of hydrometeors through a melting layer. *Proc. 13th Radar Meteor. Conf.*, Amer. Meteor. Soc., Boston, 148-153.

Simpson, J. S., and V. Wiggert, 1971: 1968 Florida cumulus seeding experiment: numerical model results. *Mon. Wea. Rev.*, 99, 87-118.